

Exploring welding parameter effects on friction stir weld joints in aluminum 8006 alloy using response surface methodology

Chakrasali Chandrakumar^{*1,a}, Irappa Sogalad^{2,b}, Arun Kumar Shettigar^{3,c}, Akash Korgal^{3,d}, Madeva Nagaral^{4,e}

¹Dept. of Mechanical Eng., Proudhadevaraya Institute of Technology, Hospet, Karnataka, India

²Dept. of Mechanical Eng., University BDT College of Engineering, Davanagere, Karnataka, India

³Dept. of Mechanical Eng., National Institute of Technology, Surathkal, Karnataka, India

⁴Aircraft Research and Design Centre, Hindustan Aeronautics Limited, Bangalore, Karnataka, India

Article Info

Abstract

Article History:

Received 29 Aug 2024

Accepted 18 Nov 2024

Keywords:

Friction stir welding;
Microhardness;
Impact toughness;
Response surface methodology;
Central composite design

This study aims to develop mathematical models that can predict the characteristics related to mechanics, such as microhardness and impact resistance, of Aluminum that has been friction stir-welded 8006 alloy joints with 95% confidence. The four process parameters tool tilt angle, welding speed, tool pin shape, and rotating speed were systematically varied across three levels. Following a response surface and central composite design approach that is face-centered, the influence of different factors on the mechanical properties of aluminum 8006 alloy joints was assessed. The highest impact toughness of 58 joules was observed in joints specially prepared by a cylindrical threaded pin profile tool with a 1° tilt angle operating at 800 RPM and a feed rate of 20 mm/min and test was conducted at room temperature. Additionally, it was investigated how process factors affected impact toughness by ANOVA and the results revealed that the tool pin geometry is identified as the most significant process variable on impact toughness, contributing 52.52%, thereafter the tool tilt angles (15.53%), rotating speed (8.80%), and welding speeds (5.84%). The findings showed that, for impact toughness, the tool tilt angle and pin shape were more important than welding speed and tool rotation speed, but the tool pin profile and the welding speed showed governance over rotational speed and angle of tilt in case of hardness. The joints achieved a maximum hardness of 166 VHN at stir zone of the welded specimen made from a threadless taper pin tool for the speed of 1200 rpm, the tool was tilted at 2 degrees while welding at a speed of 40 mm/min. Finally, the effects of process parameters on the microstructure of friction stir welded Aluminum 8006 alloys were addressed and discussed.

© 2024 MIM Research Group. All rights reserved.

1. Introduction

Exploring for lightweight materials, particularly Aluminum 8006 alloy is a promising material because of its unique combination of mechanical properties like, corrosion resistance, and lightweight nature makes an extensive variety of applications such as automotive body panels, food packaging, heat exchangers, electrical conductors, and structural components. FSW is a groundbreaking welding method that was initially developed in 1991 by Wayne Thomas of the United Kingdom's "The Welding Institute" (TWI). It is a method of solid-state welding that connects

*Corresponding author: chakrasali@pdit.ac.in

^aorcid.org/0009-0004-0618-6915; ^borcid.org/0000-0002-4475-3579; ^corcid.org/0000-0003-0273-7746;

^dorcid.org/0000-0002-6237-3983; ^eorcid.org/0000-0002-8248-7603

DOI: <http://dx.doi.org/10.17515/resm2024.424ma0829rs>

Res. Eng. Struct. Mat. Vol. x Iss. x (xxxx) xx-xx

several metal parts without melting. Wahid et al. [1] examined the performance of butt joints produced through friction stir welding of AA8011 alloy and identified that welding speed is the utmost important aspect, followed by diameter of shoulder diameter and the tool's rotating speed. Within the stir zone, the microstructure revealed tiny, equiaxed granules that had rapidly recrystallized and it exhibited a better microhardness compared to the original metal. Davidson et al. [2] They investigated how the mechanical characteristics of AA8011 alloy were affected by the friction stir welding process variables. Their findings revealed that the joint achieved a peak tensile strength of 82 MPa when produced with an axial force of 2.15 kN, the welding process employed a tool rotation speed of 1400 RPM and a feed rate of 45 mm/min. Additionally, they observed the presence of finer grains, a defect-free joint, and improved tensile strength and hardness in the stir zone. Raghuraj et al. [3] investigated the highest micro-hardness value and ultimate tensile strength which utilized a tool rotation speed of 1400 RPM, and a feed rate of 25 mm/min, and a dwell time of 7 seconds. They also observed that the rotation of the tool pin transferred material from the advancing side to the retreating side, with temperature variations being more pronounced. The influence was more significant on the retreating side than on the advancing side. Navneet et al. [4] found the highest value of 84.44 MPa tensile strength and 64.95 percent efficiency as that of base metal. Taguchi analysis was employed to optimize the tensile strength testing parameters, which were 1,500 rpm speed, 1° tilt angle, and 50 mm/min feed. The sample with outstanding tensile strength, equiaxed grain's structure, maximum temperature of 389 °C, and reaching its peak on the advancing side, nugget zone, a hardness value of 36.4 HV was found. Palani et al. [5] used a hybrid fuzzy-based response surface methodology was employed to determine the optimal process parameters for friction stir welding. The optimal parameters were found to be a rotating speed of 2050 rpm, a 90° angle of tool tilt, and a transverse speed of 40 mm/min. Additionally, the study revealed that welding speed was the primary factor affecting the toughness of the joints. In contrast, the study revealed that tool tilt angle and welding speed were the most significant contributors to Vickers microhardness. Ito et al. [6] evaluated the Vickers hardness of 7075-O raised while the 7075-T6 joints' Vickers hardness dropped in the stir zone. In contrast to the O joints, whose Vickers hardness increased even more after 5 months of natural age, the T6 joints' stir zones hardened to a point where they were almost as hard as the base material. Gao et al. [7] studied the microstructure and hardness of an aluminum 6082 alloy friction stir welded joint. The distribution of hardness followed a 'W' shape, with a base material hardness value of 103 HV, a heat-affected zone (HAZ) hardness value of 72 HV, and a nugget zone hardness value of 84 HV. The Grain microstructure and particles from the second phase were studied in different parts of the joint by Wan et al. [8]. The top joint region near the ultimate welding nugget zone has the highest microhardness of 89.4 HV. Due to significant plastic deformation, this region is known as the thermomechanical impacted zone. Essa et al. [9] investigated weld joints that showed better quality than the base metal's hardness, indicating that the hardening phase was reprecipitated in the weld zone. Average joint hardness values increased with decreasing rotational speed, and the results revealed that the microhardness profile was greatly impacted by the speed of rotation. The effect of traverse speed on hardness was small. Tariq et al. [10] examined the impact of process variables on the strength of the materials, the grain size and second phase particle size are increased with increasing the tool rotating speed. Density had minimal impact on the hardness of particles in the second phase. Bi-layered aluminum weldments' micro hardness reduced with increasing grain size according to the Hall-Petch equation. Sudhir Kumar et al. [11] explored that the weld joints were of higher quality than the base metal's hardness, which was potentially explained by the reprecipitation of the strengthening phase within the weld zone. The impact of the speed of the weld on hardness was small. Sadashiva et al. [12] explored the impact strength of the composite materials that shows the divergent behavior concerning both weld speed and feed rate during FSW and is caused by the inadequate thermal energy produced during welding at high speeds and feed rates. In general, the strength of the composites shows a substantial 60% improvement compared to the original AA2024 alloy in its cast state. Devaiah et al. [13] identified that the speed of the rotation of the tool has the greatest impact on the strength of welded joints, accounting for 53.02% of the overall effect. The tool tilt angle contributes 36.91%, while the traverse speed only contributes 6.14%. The optimal process conditions were determined to be a rotational speed of 1120 RPM, a feed rate of 70 mm/min, and a tool tilt angle of 20 degrees. Gurmeet et al. [14]

examined the joint strength of friction stir welded aluminum 6082-T6 alloy. Analysis of the tungsten inert gas welding technique showed that the welded joints displayed better mechanical qualities than the welded joints prepared from the TIG approach and included equiaxed granules that are fine. Conversely, large granules were seen in the TIG welded joints. Umasankar et al. [15] observed the generation of temperature is affected by the tool's rotational speed, with faster rotational speed resulting in increased temperature. They observed that 1100 rpm was the optimal rotational speed for achieving maximal impact strength and that friction pressure and contact length affected the weld joint strength. It was also apparent from the scanning electron microscope images that the dimples impacted the ductility quality of the welded components. Akbari et. al [16] discovered that the most important factor influencing the Si particle size, UTS, and force of composites was transverse speed. The Si particle size and B4C particle dispersion quality in the aluminum matrix of the parent material were strongly impacted by FSP variables. Asadi et.al [17] investigated that FSW annealing refines stir zone particle size and lowers microhardness. In fracture, stir zone structural integrity affects absorbed energy. The safe window for defect-free joints increased for each pin shape and rotation speed. Pin profile impacts fracture energy more than hardness and grain size. A neural network found that 309 mm/min traversal speed, 495 rev/min rotational speed, and threaded cylinder pin shape were the best compromise process parameters. Akbari et. al [18] explored input-output relationships using response surface methodology (RSM). The hybrid multi-objective optimization found the ideal probe diameter, shoulder diameter, and probe height of 5.1 mm, 17.63 mm, and 3.86 mm. The investigation found that shoulder diameter, probe diameter, and probe height most affected temperature force and failure load. Ahmadi et. al [19] experimentally conducted that the high rotating speed to welding speed ratios produce coarser and larger grains and validate welded samples' weak or strong performance. Welding speed improves Vickers microhardness and ultimate tensile strength, whereas rotational speed decreases both. The square-pin weld with 80mm/min welding and 1600 RPM rotating speeds had the highest DIC-aided fracture toughness.

Kesharawani Rahul et. al [20] studied the effect of tool design on the quality of friction stir welds (FSW), it has been observed that the use of a threaded cylindrical tool pin in friction stir welding (FSW) achieved a defect-free, uniform mixing of powder particles with the aluminum matrix and high-quality of joints. Optical micrographs, along with EDS analysis, also reveal an oxygen weight percentage of 11.35% in the stir zone (SZ) and the effective incorporation of powder particles, was confirmed in SEM images. Rahul et. al [21, 22] explored the influence of pin profiles on friction stir welded aluminum 6061-T6 alloy with Al₂O₃ particle reinforcement join. The results reported that the threaded pin profiles were enhanced the material mixing and improved the flow in the plasticized state, compared to flat pins, where the plasticized material tends to adhere to the tool pin surface and microstructural shows that the powder particles are more uniformly distributed in the stir zone (SZ) when using threaded pins, whereas agglomeration occurs with flat pins. The EBSD studies indicate that the average grain size in the SZ is finer for threaded pins (3.74 μm) compared to flat pins (5.64 μm). Additionally, the fraction of high-angle grain boundaries is higher for threaded pins, suggesting enhanced material refinement and improved weld quality. Imad et. al [23] was reported the comparison of size of reinforced particles in Al6061-matrix composites. The result shows that the significant microstructural refinement of SiC and Zn particle-reinforced Al-matrix composites, with grain sizes of 4.79 μm and 4.18 μm, respectively and also the composites exhibit improved micro hardness 130 HV for Zn, 112 HV for SiC_p. However, the higher mechanical properties, with UTS values of 224 MPa (SiC) and 236 MPa (Zn), and YS values of 155 MPa (SiC) and 172 MPa (Zn), outperforming the unreinforced AA6061-T6. However, elongation is decreased to 35% compared to 52% for the base alloy. Jha et. al [24] demonstrated the efficiency of the friction stir lap welding (FSLW) technique in creating excellent dissimilar AA6061/AA7075 joints. They found that, the defect-free interfaces were produced under these optimized parameters of 850 RPM rotational speed, and 55 mm/min of feed rate. Microstructural examination result also shows the significant grain refinement and shear textures in the stir region due to continuous dynamic recrystallization (CDRX). In spite of that some thermal softening of material reduced the micro hardness, while the SZ exhibits improved strength, ductility, and strain-hardening properties.

Considering the literature review, it is evident that numerous researchers have employed various statistical and optimization methods to identify the ideal procedure for using friction stir welding to evaluate the connection quality between various aluminum alloys. To date, a limited amount of research has explicitly focused on the friction stir processing (FSP) of the AA8006 aluminum alloy. However, there is a notable absence of systematic investigations into the microstructural and mechanical properties, including hardness and impact toughness, of AA8006 when subjected to FSW. This study hopes to fill this gap by investigating the impact of FSW on AA8006 alloy, offering novel insights into its weldability and performance attributes.

Therefore, the primary objectives of this work are to determine the optimal process parameters such as tool tilt angle, rotating speed, welding speed, and tool pin shape to achieve defect-free, strong weld joint and to establish an empirical relationship for impact toughness by using central composite design of response surface methodology (RSM). Furthermore, the study explored the impact of welding parameters on the hardness and microstructural changes in AA8006 aluminum alloy resulting from friction stir welding.

2. Experimental Procedures

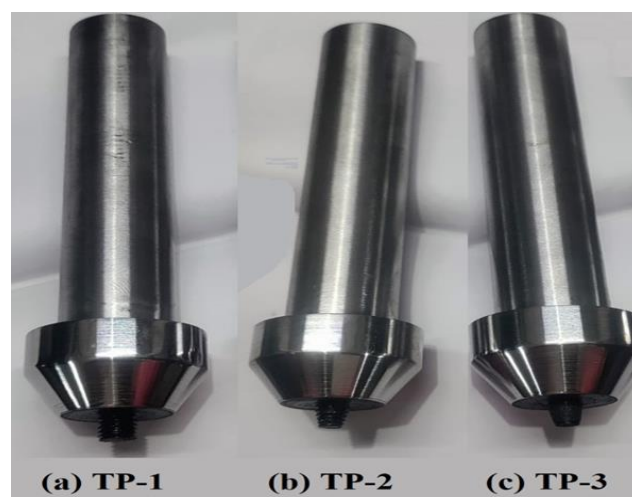
This section provides a detailed explanation of the welding parameters, experimental setup, and research methodology.

2.1. Materials and Selection of Tool

This work uses the stir casting process to fabricate a base plate made of As-cast aluminum 8006 alloy. The chemical composition used to produce aluminum 8006 alloy material is shown in Table 1. After fabrication, an EDM wire electro-discharge machine is used to cut two plates to the required dimensions of 80x60x6 mm. A friction stir welding approach is used to join the plates, using three different tool pin profiles of H13 high-speed steel. The pictorial representation of three tool pin profiles and the detailed dimensions of the tools are shown in Fig. 1. The selected cylindrical straight pin tool has a diameter of 6mm and an 18mm diameter shoulder with a flat and smooth surface design. In addition to having a nominal diameter of 6 mm, M6 thread tool pins are metric in size and contain threads that are cut with a 1 mm pitch and right-hand thread (RHT) orientation.

Table 1. Chemical constituent of aluminum 8006 alloy

Elements	Actual Value
Zinc, Zn	0.1%
Magnesium, Mg	0.1%
Manganese, Mn	0.60%
Silicon, Si	0.30%
Iron, Fe	1.6%
Copper, Cu	0.1%
Aluminium, Al	97.2%



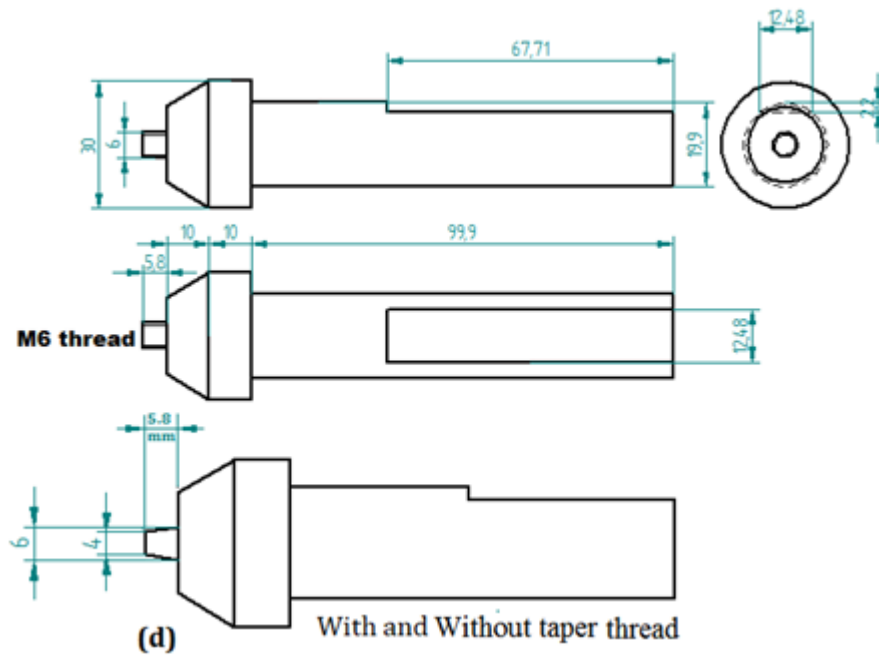


Fig. 1. Tool pin profiles: (a) TP-1: Threaded straight pin tool profile, (b) TP-2: Threaded taper pin tool profile, (c) TP-3: Threadless taper pin tool profile, (d) Dimension of Tools

2.2. Selection of Parameters

This research has employed 4 welding parameters: traverse speed, tool speed rotation, tool pin profile, and tool tilt angle. The selection process parameters are crucial because rotational speed controls heat generation, while traverse speed ensures the right balancing of heat input to form uniform microstructure and sound welds. The tool tilt angle helps in material blending and void reduction, whereas the tool pin profile influences material flow and mixing within the weld zone.

Table 2. Selected levels and variables of the process

Parameter	Symbol	Units	Levels		
			-1	0	+1
Traverse Speed	TS	mm/min	20	30	40
Rotational Speed	RS	rpm	800	1000	1200
Tool pin profile	TP	N/A	TP-1	TP-2	TP-3
Tool tilt Angle	TA	°	1°	1.5°	2°

2.3 Friction Stir Welding Technique

A computer-controlled FSW machine was used for the joint fabrication. The cast iron plate is utilized as a backing plate. Every one of the welds is 120 mm long. The workpiece was systematically labeled after every experiment. Before welding the surface of aluminum 8006 alloy plates is cleaned thoroughly to remove contaminants and ensure a pristine welding environment. Then the plates were rigidly fixed in the FSW machine using precise fixtures and clamps to maintain alignment as shown in Fig. 2.

After that, the required process parameters are entered into the computer to control the friction stir welding operation. During the FSW operation, the generation of heat due to friction between the rotating tool and material leads to the metal being in a solid-state condition. The tool then stirs the softened material, creating a seamless bond.

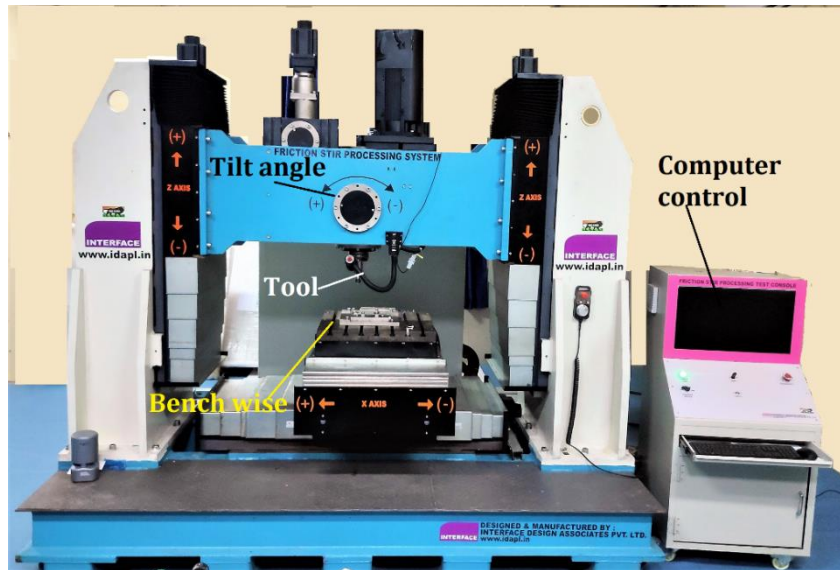


Fig. 2. Computerized friction stir welding machine setup

2.4 Preparation of FSW Specimen

The specimens for Charpy impact toughness and Vickers microhardness were prepared in a direction perpendicular to the weld. According to ASTM E23-04 standard, the impact test specimens were extracted from the welded plate to the required dimensions with the help of wire EDM, and the dimensions of prepared Charpy impact samples were revealed in Fig. 3. The notch measured 10 mm in length, 2 mm in depth, and a 45° angle. Subsequently, the specimens underwent meticulous polishing to eliminate surface flaws and ensure a fine surface finish. The specimen preparation procedure was carefully executed to ensure the precision and consistency of the impact test results.

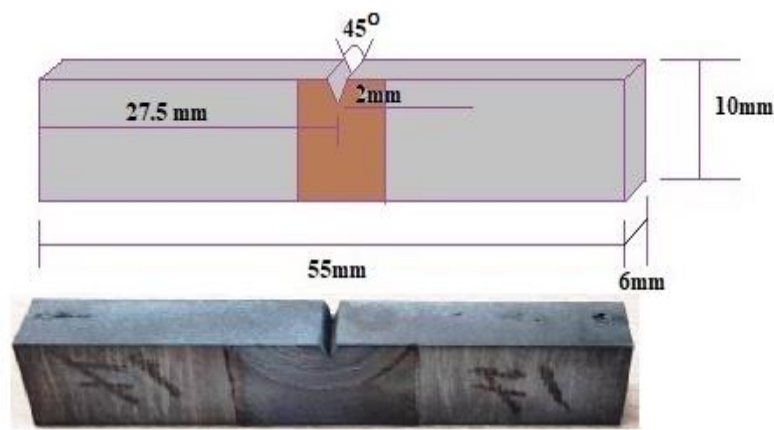


Fig. 3. Specimen dimensions for impact test

3. Statistical Analysis

The statistical analysis of friction stir welded aluminum 8006 alloy involves a systematic study of factors which as traverse rate, tool pin shape, angle of tilt, and rotation speed. ANOVA and regression analysis are used to assess the influence of these parameters on the quality of welding and mechanical characteristics.

Statistical analysis not only evaluates the consistency and reliability of FSW joints but also guides the formulation of predictive models, enabling precise control over the welding process for optimal results. To determine the optimal combination of these factors, an experimental setup is used that combines response surface methodology (RSM) with a face-centered central composite design

(CCD). Table 2 provides a detailed report of the process variables employed in the experiments, with their respective values. The central composite design uses the full factorial method, which includes three distinctive levels for each parameter.

3.1 ANOVA for Charpy Impact Toughness

ANOVA is performed on the Charpy impact strength of friction stir welding of AA8006 alloy using various welding parameters. The ANOVA evaluates the significance of these factors and their contribution to the impact strength of FSW joints. An ANOVA is used to determine the factors that have a statistically significant effect on the toughness of the welded joint by comparing the means of impact strength for various parameter values. This study helps in interpreting the most relevant variables and allows the optimization of friction stir welding (FSW) conditions to achieve enhanced Charpy impact strength in AA8006 alloy. ANOVA results reveal significant findings: the high Model F-value of 62.78 indicates the model's overall significance, confirming its relevance in explaining the impact toughness variations. Additionally, the significant Lack of Fit, indicated by the F-value of 9.08, highlights the importance of the model fit precision, highlighting the need for further adjustment in the areas where the model lacks accuracy.

Table 3. Experimental DOE with output response

Expt. No.	Input parameters				Output response	
	Rotational Speed in (RPM)	Traverse Feed (mm/min)	Angle of Tilt in (Degree)	Tool pin profile	Impact Toughness (Joule)	MHV at Nugget zone
1	800	20	1°	1	58	118
2	1200	20	1°	1	46	125
3	800	40	1°	1	44	121
4	1200	40	1°	1	42	131
5	800	20	2°	1	40	124
6	1200	20	2°	1	36	134
7	800	40	2°	1	34	130
8	1200	40	2°	1	31	142
9	800	20	1°	3	36	137
10	1200	20	1°	3	24	140
11	800	40	1°	3	28	142
12	1200	40	1°	3	18	146
13	800	20	2°	3	25	148
14	1200	20	2°	3	15	150
15	800	40	2°	3	19	152
16	1200	40	2°	3	12	166
17	800	30	1.5°	2	43	141
18	1200	30	1.5°	2	35	149
19	1000	20	1.5°	2	33	137
20	1000	40	1.5°	2	30	140
21	1000	30	1°	2	39	138
22	1000	30	2°	2	32	145
23	1000	30	1.5°	1	47	138
24	1000	30	1.5°	3	32	153
25	1000	30	1.5°	2	40	145
26	1000	30	1.5°	2	39	145
27	1000	30	1.5°	2	40	146
28	1000	30	1.5°	2	41	147
29	1000	30	1.5°	2	40	146
30	1000	30	1.5°	2	39	145
31	1000	30	1.5°	2	39	145

The ANOVA analysis of impact toughness in friction stir welded AA8006 alloy provides insights into the individual contributions of parameters on the toughness of the joint. The coefficient of determination (R^2) at 98.21% specifies that 98.21% of the variability in impact toughness is explained by the chosen parameters, affirming the model's strong fit and reliability. Furthermore, the modified R^2 , closely aligning with the projected R^2 at 96.65%, indicates that the model is appropriately constructed without unnecessary variables, ensuring its accuracy.

Statistical analysis not only evaluates the consistency and reliability of FSW joints but also guides the formulation of predictive models, enabling precise control over the welding process for optimal results. To determine the optimal combination of these factors, an experimental setup is used that combines response surface methodology (RSM) with a face-centered central composite design (CCD). Table 2 provides a detailed report of the process variables employed in the experiments, with their respective values. The central composite design uses the full factorial method, which includes three distinctive levels for each parameter. The high accuracy, shown by the proportion of signal to noise over 4 (specifically, 33.594 in this instance), underscores the model's dependability in detecting significant trends amongst the background noise in the data.

Table 4 .ANOVA Summary for Impact Strength

Source of Variation	SS	DOF	MS	F (F value)	P (P value)	% of contribution
Model	3037.54	14	216.97	62.78	< 0.0001	
RS	272.22	1	272.22	78.76	< 0.0001	8.80
TS	180.50	1	180.50	52.22	< 0.0001	5.84
TA	480.50	1	480.50	139.02	< 0.0001	15.53
TP	1624.50	1	1624.50	470.02	< 0.0001	52.52
RS*TS	20.25	1	20.25	5.86	0.0278	0.65
RS*TA	12.25	1	12.25	3.54	0.0781	0.34
RS*TP	16.00	1	16.00	4.63	0.0470	0.52
TS*TA	12.25	1	12.25	3.54	0.0781	0.34
TS*TP	4.00	1	4.00	1.16	0.2980	0.13
TA*TP	16.00	1	16.00	4.63	0.0470	0.52
RS*RS	1.73	1	1.73	0.5000	0.4897	0.056
TS*TS	115.94	1	115.94	33.55	< 0.0001	3.75
TA*TA	18.70	1	18.70	5.41	0.0335	0.60
TP*TP	4.49	1	4.49	1.30	0.2709	0.15
Residual	55.30	16	3.46			1.79
Lack of Fit	51.87	10	5.19	9.08	0.0069	significant
Pure Error	3.43	6	0.5714			
Cor Total	3092.84	30				
R^2 : 98.21%	Adjusted R^2 : 96.65%	Predicted R^2 : 90.18%				

3.2 Mathematical Regression Model

A formula in mathematics was created to ascertain the connection between welding speed, rotating speed, tool pin profile, and tool inclination angle. By analyzing experimental data, regression coefficients for a mathematical model featuring second-order polynomials were identified. To quantify the impact toughness of friction, stir-welded aluminum 8006 alloys, regression equation (1) was formulated, which can be expressed as follows:

$$\begin{aligned}
 IT = & 70.0 - 0.0730 RS + 2.926 TS + 7.0 TA - 12.64 TP - 0.0672 TS * TS \\
 & - 10.87 TA * TA + 1.28 TP * TP + 0.1500 TS * TA \\
 & + 1.750 TA * TP
 \end{aligned} \tag{1}$$

Using design expert (version 22.0.8) software, the regression model coefficients for impact toughness were determined with a 95% level of confidence. Impact toughness, or IT, is the dependent variable in the regression formula that quantifies the impact of each process variable.

The RS, TS, TA, and TP variables are the coefficients in this equation, which include linear, square, and interaction terms. The terms with positive coefficient indicate the most significant influence variable on impact toughness whereas the negative coefficient term says that the less influence on impact energy of welded joint. The above equation (1) reveals that the welding speed and angle of tool tilt are the high-impact variables, where the rotational speed and profiles of the tool pin eradicate the material toughness. The square and interaction terms have negligible effect on the impact toughness of the FSWed joint.

4 Results and Discussion

4.1 Categorization of Charpy Impact Toughness of FSWed Plates

The Charpy impact toughness test was conducted to predict how different process factors affect the impact energy of the specimen. The average impact toughness value of the samples of 31 experimental are presented in Table 3. The outcomes show that the FSWed fabricated by a straight threaded pin tool with 800 rpm rotational speed, 20mm/min traverse speed, and 1° the angle of the tool tilt gives a maximum impact strength value of 58 joules because the threaded profile aids in optimal material flow, leading to improved bonding structural integrity with a fine-grained, defect-free microstructure and energy absorption in the weld zone. Nevertheless, the threadless taper pin tool yielded the lowest impact strength measurement of 12 joules when operated at 1200 rpm, 40 mm/min traverse speed, and 2° tilt angle. This is because the threadless taper pin geometry of the tool renders the stirring and mixing processes ineffective and higher rotational speeds result in uneven and coarser microstructure due to excessive heat generation and rapid traverse [25, 26].

The ANOVA results show that the tool pin profile has a significant impact on hardness value compared to other process parameters as represented in Table 4. The percentage of contribution of the tool pin profile has the highest value of 52.52% to the overall effect. The tool tilt angle contributes 15.53% of its total, and the rotating speed and traverse speed provide contributions of just 8.80% and 5.84% respectively of its total contribution.

4.1.1 3-Dimensional Surface Plot for The Impact Toughness

The three-dimensional surface plot (from Stat-ease software) of impact toughness provides a visual representation of the intricate relationship between various parameters in friction stir welded Aluminum 8006 alloy. This plot visually translates complex data into a comprehensible form, enabling a clear understanding of how factors such as rotation speed, traverse rate, and tool profile influence impact toughness. The surface plot provides important insights into maximizing welding conditions for improved impact toughness and overall material performance by visualizing these interconnections.

Fig. 4(a) illustrates the three-dimensional surface plot of impact toughness vs rotational speed and traverse speed. As a result of the findings, the impact energy was found to decrease when the rotational speed and welding feed were elevated. The impact energy peaked at a traverse speed of 30 mm/min and a rotational speed of 800 RPM. During welding, excess heat and rapid cooling occur at the welding portion with maximum speed and feed rate, leading to low bonding strength. The interaction between the tool tilt angle and traverse speed 3-D surface plot with impact strength is shown in Fig. 4(b). The surface plot illustrates a clear trend that the impact toughness decreases as the tool tilt angle and traverse speed increase in friction stir welded AA8006 alloy. An increase in the angle of tilt results in alterations in the welding dynamic forces, impacting the grain structure and the material flow in the welding process. Also, the higher traverse speeds affect reduced heat input, disturbing the metallurgical bonding and resulting in decreased impact toughness. Fig. 4(c) shows the interaction between the tool's rotating speed and angle of tilt against impact toughness. Results reveal that 800rpm speed and 1° angle of tilt give maximum impact strength and for maximum value, both parameters negatively influence the material's ability to absorb impact energy. Fig. 4(d) demonstrates that the tool pin geometry and rotational speed were the primary

factors influencing impact toughness. The surface plot indicates that the highest impact toughness is achieved with the threaded straight pin tool produced with a welded joint, at the minimum speed.

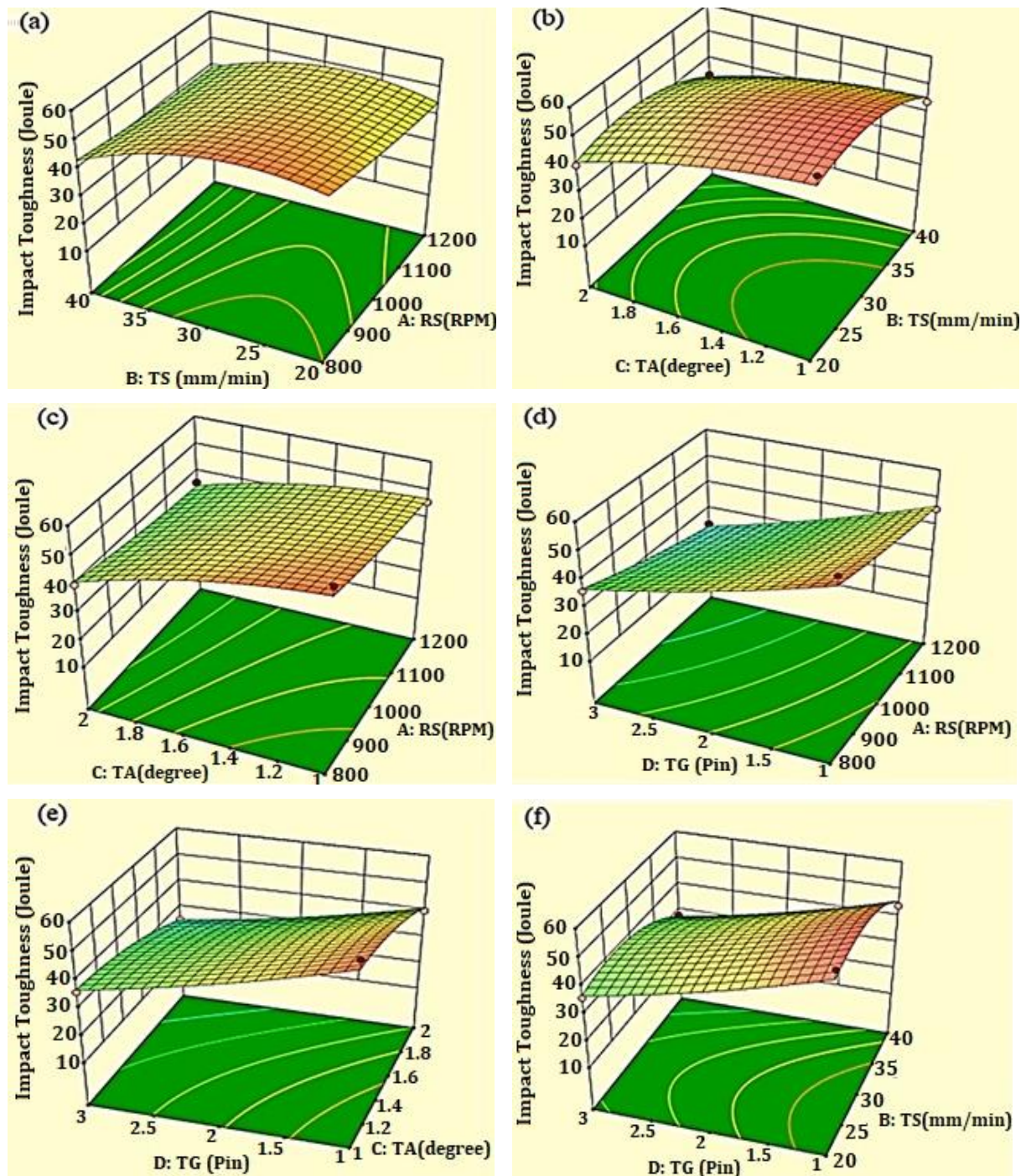


Fig. 4. Three-dimensional Surface plot of IT vs a) Traverse speed and tilt angle, b) rotational speed and speed, c) rotational speed and tool tilt angle, d) tool pin geometry and rotational speed, and e) tool pin geometry and tilt angle

The descending trend on the surface plot also indicates that increasing the rotational speed and weld with TP-2 and TP-3 tools, suggests that specific combinations of these factors compromise the mechanical properties of friction stir welded aluminum 8006 alloy. The impact toughness of the weld decreased with increasing speed in comparison to other tools' distinct pin geometries. Fig. 4(e) illustrates the influence of the tool pin design and tilt angle on toughness. For a tilt angle of 1° , the straight pip tool exhibits maximal impact toughness, which diminishes as the tool tilt angle increases. Fig. 4(f) displays the correlation between tool pin shape and traverse speed on impact energy. The results concluded the impact toughness is higher when the traverse speed increases

gradually up to 30 and with further increases in traverse speed the impact energy decreases. Insufficient heat input is unable to be provided to the weld zone is affected by the increase in welding speed. The straight thread pin will mix up the material properly and form a fine-grain structure.

4.2 Characterization of Vickers Microhardness of FSWed Plates

In the present study, according to ASTM E384, the Vickers microhardness of friction stir welded aluminum 8006 alloys has been conducted. It measures material hardness at a microscopic level to evaluate weld quality, and hardness distribution in the joint and also identifies the influence of process parameters on the materials. The Vickers digital microhardness testing machine was used. This test is based on the principle of measuring the diagonal lengths of an indentation made by a diamond-shaped indent.



Fig. 5. Vickers Microhardness testing machine

Before the testing, the specimens were polished and finished to get a clear mirror image using a fine 800-grade emery paper and to avoid errors during the experiments. The specimen's microhardness was measured at several locations on plates positioned 2mm apart, ranging from the center of the weld to the margins of the plate. The welding center acted as the stir zone, which refers to the area subjected to heat and mechanical force from the tooltip. This area is often referred to as the zone affected by thermomechanical factors. The zone impacted by heat was located next to the welded region, where it was exposed to heat generated by the FSW process. The extreme area was an unaffected zone that was the utmost edge of the plates. By applying a 500gf load for a specific dwell time of 15 sec at room temperature, the indenter creates an impression on the material surface. The hardness values are recorded from the digital display of the Vickers microhardness testing machine (model: HVS-1000DN) as presented in Fig. 5. The recorded microhardness values are presented in Table 3.

Fig. 6 shows the contour plot (from Origin2023b SR1 student version) of the microhardness profile of 31 friction stir welded AA8006 alloy specimens under several process parameters. The different regions are identified from the welded region. The central part of the welded region as indicated in the red line shown in Fig. 6 is referred to as the Nugget Zone (NZ). In this region, the instant heat is generated by the stirring action of the tool due to which material undergoes plastic deformation. This is the origin distance from which other regions are referenced at equidistance on either side of the welded region. The zone that is impacted by both mechanical and thermal effects but less intense which was present in surrounding the NZ known as the TMAZ, and it is located 2 mm onward on either side of NZ indicated by green lines. The heat-affected zone (HAZ), considered to be at a distance of 4mm from TMAZ, is the region affected by the heating of the base material as shown in blue lines. The next to the remaining portion of the HAZ zone is called the base metal (BM) zone where the material will not experience the heating effect as illustrated in blue color. It indicates from the contour plot that NZ has a high hardness value in all the specimens tested because the metal faces thrust and rotational friction forces from the shoulder, alongside shear

stress and rotational friction from the tool pin. Under plastic deformation, frictional heat, and swirl action, broken grains must undergo dynamic recovery and recrystallization [27].

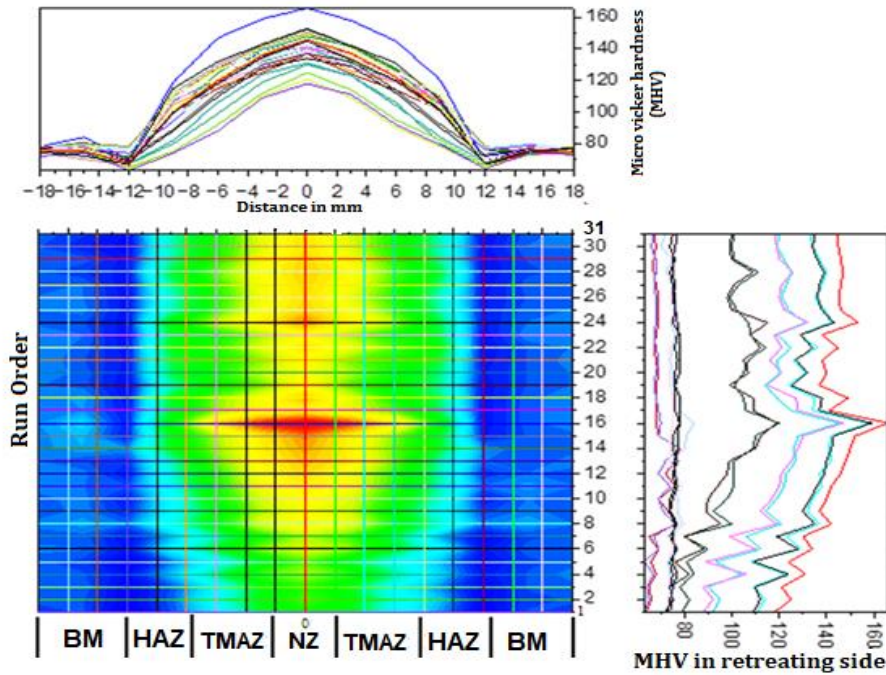


Fig. 6. Contour plot representation of microhardness distribution for 31 test specimens at different regions

In NZ, the increase of recrystallization grains is not of great importance. Thus, it is evident that the NZ microstructure has a homogeneous grain size distribution with small, equiaxed grains that are smaller than those in the base metal (BM) as shown in Fig. 8. The highest hardness value is obtained when the rotating speed of the tool increases as indicated by Fig.7. The run order 16 test specimens had a maximum hardness value of 166 VHN. Regardless of rotational speed, welding speed, tilt angle, and tool profile, all experimental runs consistently showed that the hardness of the nugget zone (NZ) in friction stir welded aluminum 8006 alloys is significantly greater than that of the base metal, as indicated at the top of the contour plot. This occurs because, in the process of friction stir welding, the material undergoes substantial plastic deformation and suffers high strain rates as a result of the stirring action of the revolving tool.

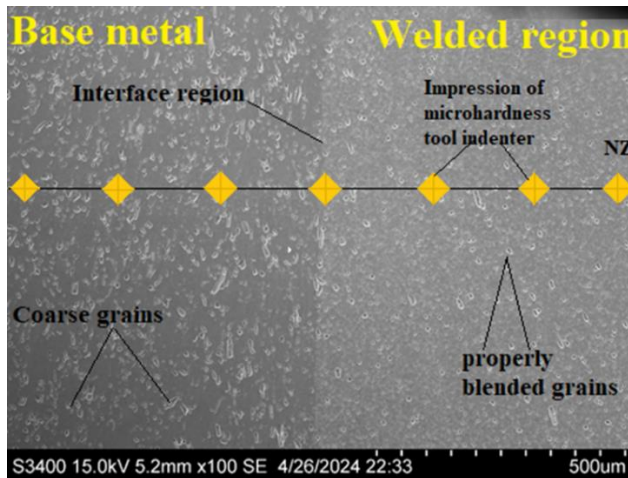


Fig. 7. SEM microstructure of top surface of FSW specimen

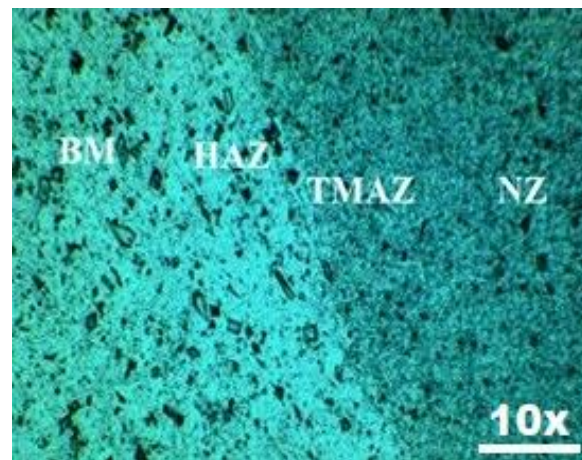


Fig. 8. Microstructure of various zones in FSWed metal

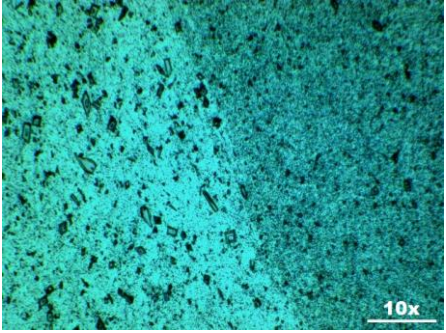
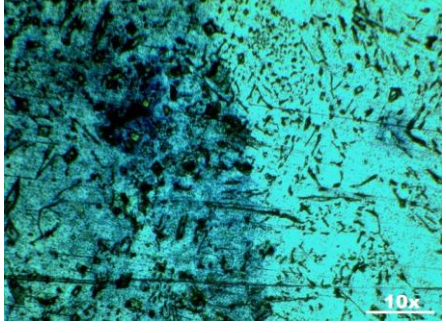
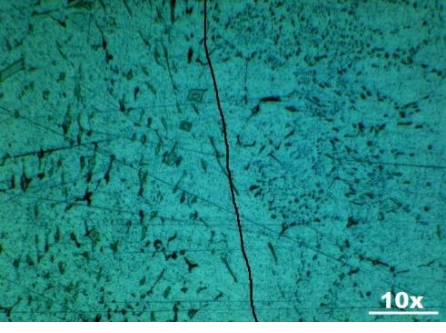
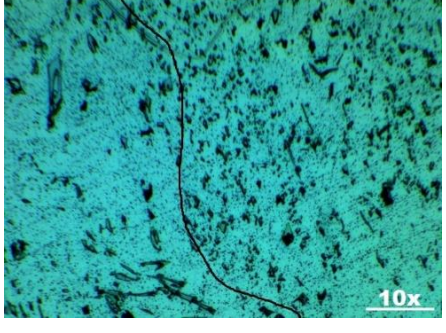
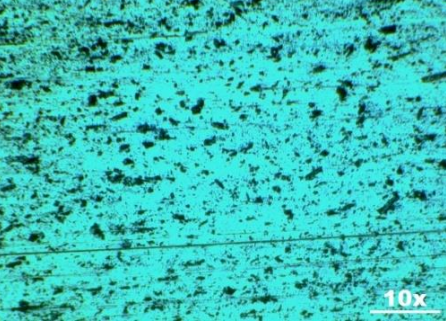
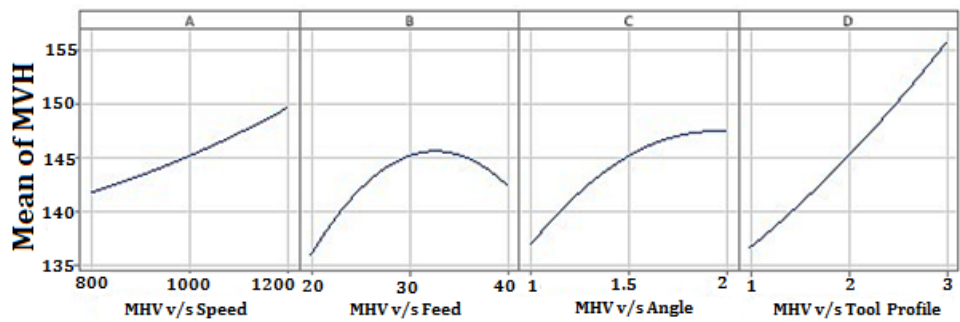
Sl. No	Run order	Process Parameters	Microscopic Image analyzer with Magnification
01	1	1200rpm, 40mm/min,1°, TP-3	
02	5	800rpm, 20mm/min, 2°, TP-1	
03	9	1200rpm, 40mm/min, 2°, TP-1	
04	15	1000rpm, 30mm/min, 2°, TP-2	
05	25	1200rpm, 40mm/min, 2°, TP-3	

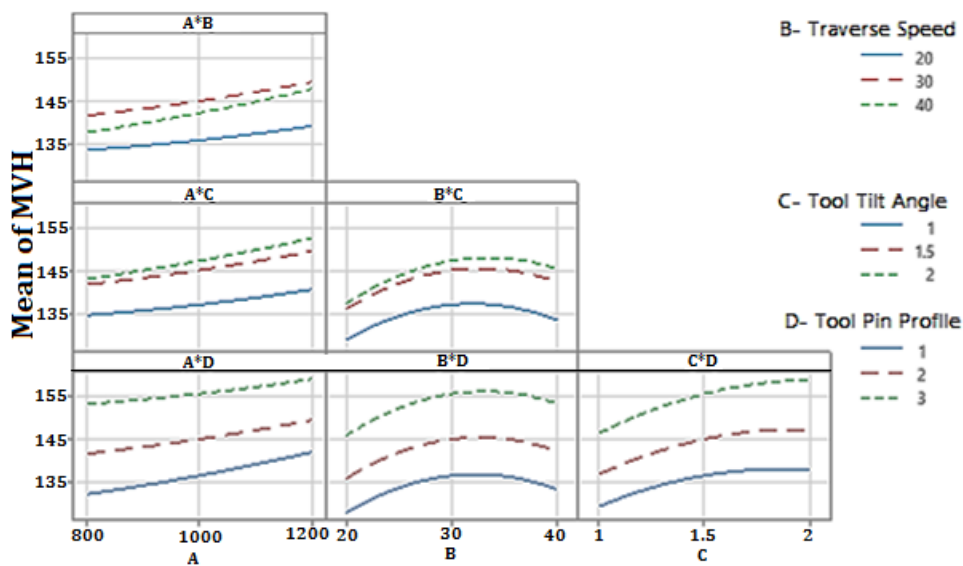
Fig. 9. Image analyzer microstructure of different FS welded specimens

In the metallographic investigation of aluminum 8006 alloys, Keller's Reagent was frequently employed as the etchant. The solution was formulated by combining 5 mL of Nitric Acid (HNO₃), 3 mL of Hydrochloric Acid (HCl), 2.0 mL of Hydrofluoric Acid (HF), and 190 mL of distilled water. The acids were incrementally introduced to the water while maintaining constant agitation to guarantee thorough mixing. The polished aluminum specimen was subsequently etched by immersing it in Keller's Mixture or spreading the solution with a brush for 10 to 30 seconds, contingent upon the desired etch depth. After etching, the sample was washed with distilled water and ethanol to arrest the chemical process and avoid over-etching. Ultimately, it was dried using warm air before microscopic analysis. This technique clarified the edges of grains, and flaws within the microstructure of the aluminum 8006 alloy as shown in Fig. 9.

The material undergoes recrystallization as it passes through the plastic stage. As demonstrated in microstructure Fig. 8, recrystallization causes new, smaller grains to develop in the base metal, replacing the earlier, bigger grains. The nugget zone experiences an increase in hardness because of the presence of these extremely small recrystallized grains. Higher material hardness is produced by the greater grain boundaries that smaller grains usually have, which prevent dislocation movement [28]. TMAZ is the name of the area next to NZ. Because the material flow generated plastic shear stress, the material in the nugget zone deforms plastically; recrystallization does not take place in the TMAZ. Moreover, heat from the stir zone has a minor impact on the substance. For this reason, the grains in this area elongated in the direction of the highest shear stress. The top section's granules are extended downward. The heat-cycle-influenced zone that does not undergo plastic deformation known as the HAZ, is the next section of the TMAZ. The structure is similar to base material because the grains are coarser. when the base metal experiences neither a heat cycle nor mechanical deformation [29].



(a) Main effective plot for MHV



(b) Interaction plot for MHV

Fig. 10. (a)Main effective plot, (b) Interaction plot for MHV

The right side of the contour plot in Fig. 6 also reveals how the hardness values were changed concerning the run order of the experiments towards the retreating side. At the NZ, the threadless taper pin tool in experimental run number 16 has a maximum hardness value and a decreasing hardness value as it shifts from the nugget zone (NZ) toward the base material's boundary. The tool has a 1200 rpm rotating speed, a 40 mm/min traversal speed, and a 2° tilt angle. Similarly, excluding run order 16, all run order values' hardness gradually decreased irrespective of process parameters. Figure 10 shows the main and interaction plots (from the Minitab 21.1.0.0 version) for the microhardness value. A threadless taper pin profile tool's hardness rises in tandem with its traverse speed, rotating speed, and angle of tilt. But behind 30 mm/min traverse speed, the hardness value decreases gradually, as represented in Figure 10(a). The effect of the interaction of process variables on MHV is illustrated in Figure 10(b), which shows that the traverse speed to the angle of tilt has the minimum effect on the material's microhardness as compared with other variables.

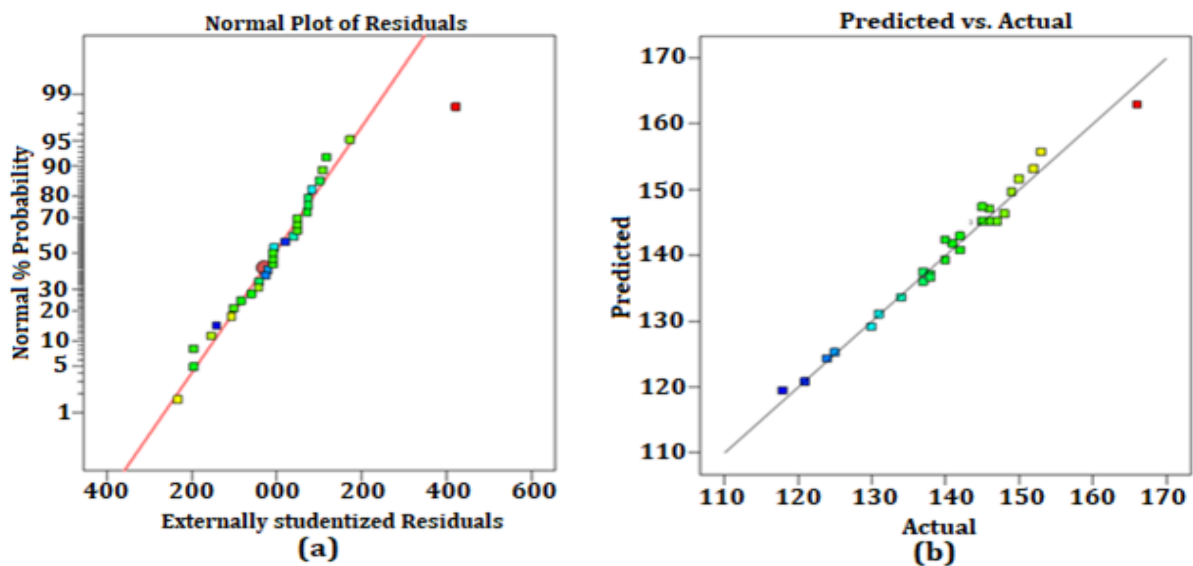


Fig. 11. Response of (a) residual vs normal % probability, (b) Predicted vs Actual

The response plot of normal % probability versus externally studentized residuals is shown in Figure 11(a). The externally standardized residuals' normal probability plot shows that the errors are generally distributed as they align closely with the straight line. The microhardness values, as indicated by Fig. 11(b), illustrate that the projected model has high accuracy since the predicted and actual values fall within extremely small deviations from their respective straight lines.

4.3 Optimization

The Response Surface Methodology's goal is to identify the ideal factor values that maximize response. Table 5 provides a summary of the optimization's outcomes.

Table 5. Optimized process parameters, their levels, and response

Process Parameters	Impact Toughness	Microhardness value
Rotating speed	800 rpm	1200 rpm
welding speed	20 mm/min	40 mm/min
The angle of tilt	1°	3°
Profile of tool pin	Threaded straight-pin tool	Threadless taper pin tool
Output response value	58 Joules	166 MHV

5. Conclusions

The mechanical attributes, like impact toughness and microhardness, were examined utilizing a central composite design and response surface approach after aluminum 8006 alloy was joined using FSW. The mechanical properties of the welded joints were evaluated using empirical equations. The following conclusions were drawn from the study's findings:

- A robust mathematical model for predicting mechanical characteristics, specifically impact toughness in friction stir-welded aluminum 8006 alloys, was established using a central composite design of response surface methodology.
- The mathematical model successfully improved the impact toughness of the material by identifying the best combination of process conditions, including tool pin profile, rotational speed, welding speed, and tool tilt angle.
- The tool pin shape was found to be a major influencing factor on the impact strength of the FS-welded joints. Threaded straight cylindrical threaded pin profile tool demonstrated the highest impact toughness as compared to other tool pin profiles.
- The maximum impact toughness of 58 joules was achieved with a straight cylindrical threaded pin profile tool, a rotation speed of 800 rpm, a welding speed of 20 mm/min, and a tool tilt angle of 1°.
- ANOVA results identified that the profile of the tool pin has the highest significant influence on the impact strength of welded joints, contributing 52.52% to the overall effect. The tool tilt angle accounts for 15.53%, but the rotating speed and traverse speed provide just 8.80% and 5.84% respectively.
- The hardness of the FSW aluminum 8006 alloy joints varies by location. The hardness value reduces as the tool proceeds from the nugget zone to the edge of the base material. However, the highest hardness is observed in the nugget zone, as the weld zone experiences an increase in hardness, which may also lead to increased brittleness. The optimal parameters for these observations were a tilt angle of 2°, a rotational speed of 1200 rpm, and a welding speed of 40 mm/min.
- The hardness development in friction stir welding samples relatively improved Vickers microhardness of 166 VHN as compared to a base material, and other methods at the stir zone for straight cylindrical threaded pin tool.
- The contour plots indicate that microhardness values were the highest value at the stir zone and as it moves towards base metal the microhardness decreases gradually and forms a 'W' shape structure.
- Microstructure from image analyzer represents that higher value process parameters form very fine grain structures as compared to lower-level parameter values.

Acknowledgment

We heartily express our gratitude to the RYMEC, Ballari for their assistance and resources that contributed significantly to the success of this study.

References

- [1] Wahid MA, Sharma N, Goel P, et al. Friction stir welding of AA 8011: mechanical and microstructure behavior. Trends in Manufacturing Processes: Select Proceedings of ICFTMM 2018, 2020; 129-138. https://doi.org/10.1007/978-981-32-9099-0_14
- [2] Davidson BS, Neelakrishnan S. Influence of friction stir welding parameters on tensile properties of AA8011 aluminum alloy plate. Journal of Computational and Theoretical Nanoscience, 2018; 15: 93-98. <https://doi.org/10.1166/jctn.2018.7060>
- [3] Panwar R, Chandna P. An experimental investigation of Al-Li alloy 8090 joint fabricated with friction stir welding (FSW) process by Taguchi-based DOE, for predicting thermal behavior, mechanical and metallurgical characteristics. Ilkogretim Online; 20.
- [4] Khanna N, Bharati M, Sharma P, et al. Design-of-experiments application in the friction stir welding of aluminium alloy AA 8011-h14 for structural application. Multidiscipline Modeling in Materials and Structures, 2020; 16: 606-622. <https://doi.org/10.1108/MMMS-07-2019-0130>
- [5] Palani K, Elanchezian C, Ramnath BV, et al. Hybrid Fuzzy based response surface optimization of welding parameters on Vickers microhardness and impact strength of FSWed AA8011-H24 aluminum alloy joints. Materials Today: Proceedings, 2020; 23: 573-582. <https://doi.org/10.1016/j.matpr.2019.05.412>
- [6] Ito T, Goloborodko A, Motohashi Y, et al. Metallurgical factors affection Vickers hardness of friction stir welded joint of 7075 aluminum alloy. Keikinzo, 2010; 60: 275-281. <https://doi.org/10.2464/jilm.60.275>

- [7] Gao KY, Li B, Ding YS, et al. Investigations on the Hardness Distribution and Microstructure of Friction-Stir-Welded 6082 Aluminum Alloy. In: Materials Science Forum. Trans Tech Publ, 2020, pp. 116-122. <https://doi.org/10.4028/www.scientific.net/MSF.993.116>
- [8] Wan L, Huang Y, Lv Z, et al. Effect of self-support friction stir welding on microstructure and microhardness of 6082-T6 aluminum alloy joint. Materials & Design 2014; 55: 197-203. <https://doi.org/10.1016/j.matdes.2013.09.073>
- [9] Essa GMF, Zakria HM, Mahmoud TS, et al. Microstructure examination and microhardness of friction stir welded joint of (AA7020-O) after PWHT. HBRC journal, 2018; 14: 22-28. <https://doi.org/10.1016/j.hbrcj.2015.05.002>
- [10] Tariq M, Khan I, Hussain G, et al. Microstructure and micro-hardness analysis of friction stir welded bi-layered laminated aluminum sheets. International Journal of Lightweight Materials and Manufacture, 2019; 2: 123-130. <https://doi.org/10.1016/j.ijlmm.2019.04.010>
- [11] Kumar S, Kumar P. Study the effect of parameters of friction stir welding on the impact strength of aluminium 6063. International Journal of Current Engineering and Technology, 2016; 6: 993-998.
- [12] Sadashiva M, Shivanand HK. Characteristic investigation on impact strength of aluminium based hybrid composite plates weld by FSW. International Journal Engineering and Technology, 2018; 7: 120-127. <https://doi.org/10.14419/ijet.v7i3.12.15891>
- [13] Devaiah D, Kishore K, Laxminarayana P. Study the process parametric influence on impact strength of friction stir welding of dissimilar aluminum alloys (aa5083 and aa6061) using Taguchi technique, International Advance Research Journal Science Engineering Technology, 2016; 3: 15303-15310.
- [14] Singh G, Kang AS, Singh K, et al. Experimental comparison of friction stir welding process and TIG welding process for 6082-T6 Aluminium alloy. materials today: proceedings, 2017; 4: 3590-3600. <https://doi.org/10.1016/j.matpr.2017.02.251>
- [15] Das U, Toppo V. Effect of tool rotational speed on temperature and impact strength of friction stir welded joint of two dissimilar aluminum alloys. Materials Today: Proceedings, 2018; 5: 6170-6175. <https://doi.org/10.1016/j.matpr.2017.12.223>
- [16] Akbari M, Asadi P, Aliha MRM, Et Al. Modeling and optimization of process parameters of the piston alloy-based composite produced by FSP using response surface methodology. Surface Review and Letters, 2023; 30: 2350041. <https://doi.org/10.1142/S0218625X23500415>
- [17] Asadi P, Aliha MRM, Akbari M, Et Al. Multivariate optimization of mechanical and microstructural properties of welded joints by FSW method. Engineering Failure Analysis, 2022; 140: 106528. <https://doi.org/10.1016/j.engfailanal.2022.106528>
- [18] Akbari M, Rahimi Asiabarak H. Modeling and optimization of tool parameters in friction stir lap joining of aluminum using RSM And NSGA II. Welding International, 2023; 37: 21-33. <https://doi.org/10.1080/09507116.2022.2164530>
- [19] Ahmadi M, Pahlavani M, Rahmatabadi D, Et Al. An exhaustive evaluation of fracture toughness, microstructure, and mechanical characteristics of friction stir welded al6061 alloy and parameter model fitting using response surface methodology. Journal of Materials Engineering and Performance, 2022; 1-19. <https://doi.org/10.1007/s11665-021-06461-1>
- [20] Kesharwani R, Jha KK, Anshari MdAA, Imam M, Sarkar C. Comparison of microstructure, texture, and mechanical properties of the SQ and thread pin profile FSW joint of AA6061-T6 with Al2O3 particle reinforcement. Materials Today Communications, 2022 Dec; 33: 104785. <https://doi.org/10.1016/j.mtcomm.2022.104785>
- [21] Kesharwani R, Jha KK, Imam M, Sarkar C, Barsoum I. Comparison of microstructural, texture and mechanical properties of SiC and Zn particle reinforced FSW 6061-T6 aluminium alloy. Journal of Materials Research and Technology, 2023; 26: 3301-21. <https://doi.org/10.1016/j.jmrt.2023.08.161>
- [22] Rahul Kesharwani, Jha KK, Imam M, Sarkar C. Multiphysics computational modelling and experimental analysis of friction stir welding of aluminium alloy metal matrix composites (AAMMCs). Engineering Failure Analysis, 2024; 108893-3. <https://doi.org/10.1016/j.engfailanal.2024.108893>
- [23] Rahul Kesharwani, Kishor Kumar Jha, Imam M, Sarkar C, Barsoum I. Correlation of microstructure, texture, and mechanical properties of friction stir welded Joints of AA7075-T6 plates using a flat tool pin profile. Heliyon, 2024; e25449-9. <https://doi.org/10.1016/j.heliyon.2024.e25449>
- [24] Jha KK, Rahul Kesharwani, Imam M. Investigation on microstructural evolution and local mechanical performance of friction stir lap welded AA6061-T6/ AA7075-T6 joints. Engineering Failure Analysis, 2024; 160: 108258-8. <https://doi.org/10.1016/j.engfailanal.2024.108258>
- [25] Venugopal V, Singh VP, Kuriachen B, et al. Effect of Process Parameters and Tool Pin Profiles on Microstructural Evolution and Mechanical Properties of Friction Stir Welded AA5052. Arabian Journal for Science and Engineering. Epub ahead of print, 2024. DOI: 10.1007/s13369-024-09714-y. <https://doi.org/10.1007/s13369-024-09714-y>
- [26] Sabari SS, Malarvizhi S, Balasubramanian V. The effect of pin profiles on the microstructure and mechanical properties of underwater friction stir welded AA2519-T87 aluminium alloy. International

Journal of Mechanical and Materials Engineering, 2016; 11: 5. <https://doi.org/10.1186/s40712-016-0058-y>

- [27] D'Souza AD, Rao SS, Herbert MA. Evaluation of Microstructure, Hardness and Mechanical Properties of Friction Stir Welded Al-Ce-Si-Mg Aluminium Alloy. *Metals and Materials International*, 2020; 26: 1394-1403. <https://doi.org/10.1007/s12540-019-00372-6>
- [28] Prabhu S, Shettigar AK, Rao K, et al. Influence of welding process parameters on microstructure and mechanical properties of friction stir welded aluminium matrix composite. *Materials Science Forum*, 2017; 880: 50-53. <https://doi.org/10.4028/www.scientific.net/MSF.880.50>
- [29] Kumar A, Veeresh Nayak C, Herbert MA, et al. Microstructure and hardness of friction stir welded aluminium-copper matrix-based composite reinforced with 10 wt-% SiCp. *Materials Research Innovations*, 2014; 18: S6-84. <https://doi.org/10.1179/1432891714Z.0000000001016>